

## The bright quasar 3C 273

Thierry J.-L. Courvoisier

INTEGRAL Science Data Centre and Geneva Observatory, 16, Ch. d'Ecogia, CH-1290 Versoix, Switzerland

Received: 5 June 1998

**Abstract.** We review the observed properties of the bright quasar 3C 273 and discuss the implications of these observations for the emission processes and in view of gaining a more global understanding of the object.

Continuum and line emission are discussed. The emission from the radio domain to gamma rays are reviewed. Emphasis is given to variability studies across the spectrum as a means to gain some understanding on the relationships between the emission components.

3C 273 has a small scale jet and a large scale jet. The properties of these jets are described. It is also attempted to relate the activity in the small scale jet to that observed in the radio and infrared continuum.

### 1. Introduction

3C 273 is the brightest quasar on the celestial sphere. This would suffice to qualify it to be the object of intense study over the years since the discovery of quasars in 1963. In addition, however, 3C 273 displays most if not all the phenomena that make Active Galactic Nuclei (AGN) such intriguing objects. Indeed, 3C 273 is a radio loud quasar that shows large flux variations at all wavelengths and at some epochs a non negligible polarization. 3C 273 has a small scale jet, the features of which move away from the core at velocities apparently larger than the speed of light and a radio structure that extends to large distances. Whether this makes 3C 273 an archetype of AGN in general or merely a very special case is left to the reader to assess. What is certain, though, is that the study of 3C 273 is relevant to all the AGN physics. The study of 3C 273 has therefore been very actively pursued over more than 3 decades.

This study has been further made easier by the position of 3C 273 very close to the celestial equator. This means that the object can be (and has been extensively) observed with the most appropriate instruments located as far North as Finland and as far South as Chile. This privileged position on the sky has the only disadvantage that the Sun comes close to 3C 273 on the celestial sphere during the year, hence hampering regularly the observations.

We will review in the next pages the early work on 3C 273, analyse then the existing data on the continuum and line emission including their variations. We will then discuss the jet which is observed at small and large distances from the core.

The host galaxy and environment will also be described. Some of the efforts made to understand the physical nature of emission components and the quasar itself will be presented.

This review is written shortly after the switch off of the International Ultraviolet Explorer (IUE) satellite which has been one of the main research instruments for AGN in recent years. It is therefore timely, as it ought to be possible to summarize the knowledge we have including all the IUE data. Large sets of data in other wave bands have been obtained in a coordinated way while IUE was taking observations, as shown in Fig. 1. Some discussions of these data and in particular cross correlations between the light curves in different bands are included in the present review, although the work is still on-going. It will be seen that it is difficult to understand all these data in a consistent way.

The equatorial coordinates of 3C 273 are  $\alpha_{2000} = 12\text{ h } 29\text{ m } 06.7\text{ s}$ ,  $\delta_{2000} = +02^{\circ}03'08''$ . The galactic coordinate of the quasar are  $l = 289.95$  and  $b = +64.36$ . The V magnitude (average) is 12.9. 3C 273 is therefore a high galactic latitude object, a clear advantage to minimize the effects of gas and dust along the line of sight. The redshift of 3C 273 is  $z = 0.158$  (Veron-Cetty & Veron 1995).

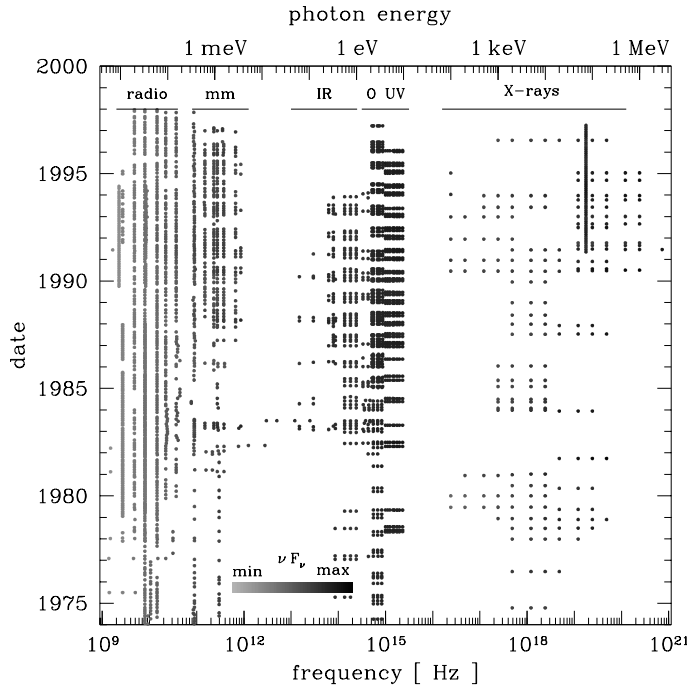


**Fig. 1.** The flux per logarithmic frequency interval  $\nu \cdot f_\nu$  is grey coded for all the frequencies and all the epochs since 1975 for which data available to us have been obtained. (From Türlér et al. in preparation, see Sect. 3). This figure shows the vast amount of data that have been gathered but illustrates also that most of the  $\nu \times$  epoch plane is not covered. A good understanding of the object would allow us to confidently extrapolate the observed data to fill the gaps. This understanding is not available yet.

## 2. Discovery and early work

3C 273 is the second radio source identified with a stellar object (Hazard MacKey & Shimmins 1963) and the first for which the emission lines were identified with a redshifted Hydrogen sequence (Schmidt 1963). It was immediately clear that if the redshift is a measure of the distance to the object its luminosity must be extraordinarily large. (Schmidt 1963) already recognized the presence of a faint jet-like nebulosity. Early work on quasars has been summarized in (Burbidge 1967) and 2 years later by (Schmidt 1969).

Early spectroscopic work interpreted the emission lines already identified in the frame of the then familiar gaseous nebulae theory (Greenstein & Schmidt 1964). These authors found that the line emitting gas must have a temperature of the order of 17 000 K and electron densities around  $10^6 \text{cm}^{-3}$ . It must be stressed that there was then no distinction between the narrow and broad line regions. These interpretations made it clear that the heavy element abundances must be close to the values found in galactic nebulae, hence close to those found in young stars. This was soon found to be a problem if the objects were to be at the cosmological distances suggested by their redshifts (Shklovsky 1964). Indeed in this case it was recognized that the light emitted by quasars must have originated when they were very young and it was not expected then that extensive stellar nucleosynthesis takes place in so short a time after the formation of structures in the expanding Universe. It now seems well established that star formation is closely associated with the process of accretion of matter from the galaxies to the very central regions in which nuclear activity takes place. Thus explaining why no nuclear activity involving only Hydrogen and Helium is observed.

Soon after the discovery of 3C 273 as an unusual object existing plate collections were used to obtain light curves. Using the Harvard (Smith & Hogleit 1963) and Pulkovo (Sharov & Efremov 1963) plate collections it was then realised that the object had varied by a factor of approximately 2 in the course of the preceding decades, although no such variations had been observed with the then modern data. Radio flux variations were also soon found in one of the components of 3C 273 (Dent 1965).

It was also noted early that the continuum spectral energy distribution of 3C 273 (and Seyfert galaxies) might cover all the known bands of the observable electromagnetic spectrum. The emission is such that roughly the same amount of energy is observed in the different parts of the spectrum. This remark followed the possible detection of X-rays from 3C 273 reported by (Friedman & Byram 1967) and the observation of an important infrared flux (Pacholczyk & Weymann 1968).

The main observational pieces of the problems posed by quasars (extreme luminosity, variability and hence compactness and emission covering most of the observable electromagnetic spectrum) were thus in place in a very short time after the first identification of point like radio sources with red shifted optical sources.

The very unusual properties of 3C 273 and a few other quasi stellar sources as compared to any of the astrophysical objects then known (stars, nebulae, supernovae etc) provoked a wide variety of possible explanations summarized in (Burbidge & Burbidge 1967). The necessity to use concepts very different from those related to nuclear processes to explain the energy requirements of Quasi Stellar Objects (QSOs), if these are at the distances implied by their redshifts, even led to alternative ideas to explain the redshifts. These interpretations became less and less plausible when the association of AGN and quasars with galaxies in which the emission and absorption line redshifts coincide and when absorption lines due to intervening matter

also at cosmological distance were discovered. It became more and more evident then that the energy released by matter when it is accreted into the very deep potential well associated with supermassive black holes is at the origin of the QSO phenomena. This idea had first been suggested by (Zel'dovich & Novikov 1964) and (Salpeter 1964) and has since then become the paradigm in which the theory of Active Galactic Nuclei (AGN) develops.

### 3. Continuum emission

The emission in the different bands of the electro-magnetic spectrum is described in this section, both spectral information and variability are discussed. Figures 2 and 3 give a representative subset of the light curves on which the description of variability is based. These curves are cuts at given frequencies of the data presented in Fig. 1. We give at the end of the section the average overall spectral distribution (the projection of the data in Fig. 1 on the frequency axis). The data shown in Fig. 1 were collected by several groups, they will be described in some details in (Türler et al. 1998) and made available on the web. In the following, data used and not specifically referenced will be drawn from this collection.

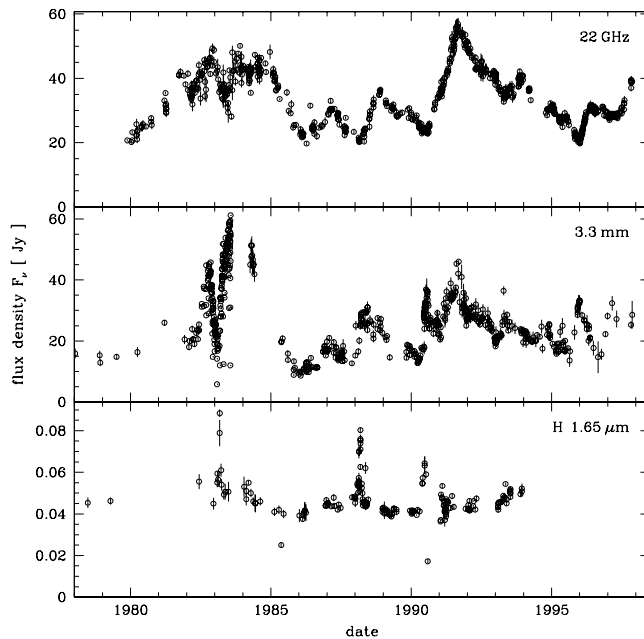


**Fig. 2.** Light curves (flux as a function of time) for a representative set of frequencies in the radio to infrared bands. These curves are (up to a factor  $\nu$ ) vertical cuts through Fig. 1.

#### 3.1. Radio emission

Low frequency (between 4.8 and 14.5 GHz) radio observations of several quasars including 3C 273 have been performed regularly at the University of Michigan

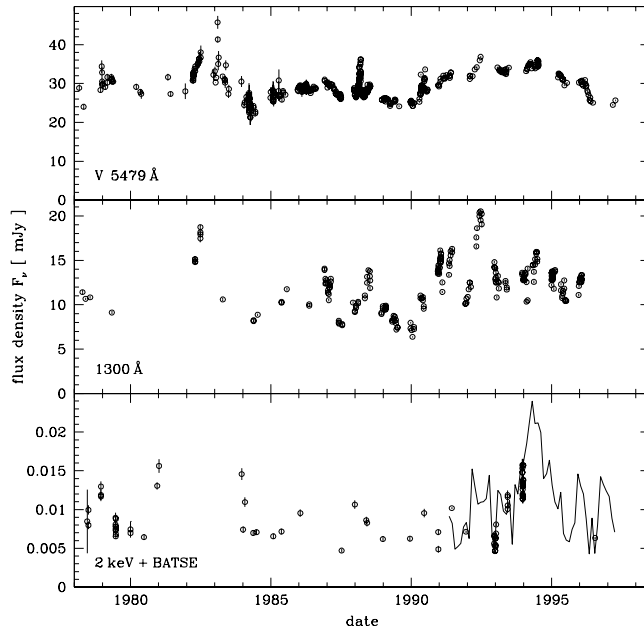


**Fig. 3.** Light curves in the visible ultraviolet and X-ray bands. Data from Fig. 1. The solid line in the lower panel is an extrapolation to 2 keV of the BATSE light curve using an average spectral index.

Radio Astronomy Observatory (UMRAO). These data have been described by (Aller et al. 1985). A further low frequency monitoring (2.7 and 8.1 GHz) from 1979 to 1987 is presented in (Waltman et al. 1991). The main characteristics of the low frequency emission are a flux of about 40 Jy at 8 GHz with 2% linear polarization. The light curve shows a broad minimum that lasted approximately 2 years around 1980. At 14.5 GHz the flux decreased by a factor 2 at the deepest point.

The variability in this frequency domain is further analysed in (Hughes et al. 1992) in terms of structure functions. It is possible to measure, using structure functions, the longest time on which variability occurs. The structure function

$$S(\tau) = \langle (f(t+\tau) - f(t))^2 \rangle = \frac{1}{N} \sum_{i=1}^N (f(t_i + \tau) - f(t_i))^2,$$

$N$  being the number of observations and  $t_i$  the epoch of each observation, is given by the average of the square of the difference of fluxes ( $f$ ) observed at two epochs separated by  $\tau$ . The structure function thus increases as a function of  $\tau$  as long as  $\tau$  is less than the maximum timescale on which the source varies. Beyond this maximum timescale the structure function is flat, and reflects the square of the amplitude of variations. In the case of 3C 273, the low frequency emission variability is such that the longest relevant time scale is longer than the data span available for the analysis, i.e. longer than 10 years.

At higher frequencies (from 22 to 87 GHz) a dense and regular monitoring of a sample of active nuclei including 3C 273 is performed at the Metsähovi Radio Research Station. This data set is described in (Teräsraanta et al. 1992). Radio emission

at these frequencies shows an increase in the amplitude of the variations as compared to the lower frequencies. At 22 and 37 GHz, the flux varies between 20 Jy and 60 Jy. This amplitude is indeed larger than the factor 2 variability observed at lower frequencies. There are no periods during which the radio emission can be described as "quiescent" onto which "flares" would be superimposed. Rather, variation is the rule and not the exception.

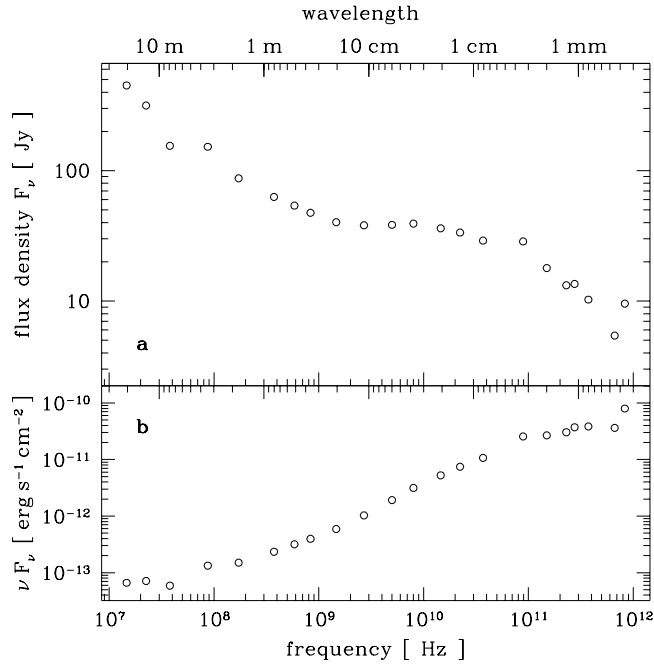


**Fig. 4.** The average radio-millimetre spectrum. Data from Fig. 1. Top panel gives the flux density  $f_\nu$  while the bottom panel gives  $\nu \cdot f_\nu$ , the flux per (natural) logarithmic frequency interval.

The non thermal character of the radio emission evidenced by the spectral energy distribution (see Fig. 4), the strong variability observed at high radio frequencies and the polarization of the flux are three elements that undoubtedly identify the radio emission mechanism as synchrotron radiation. The variability of the sources is one of the main elements to postulate that the relativistic electrons emitting the synchrotron radiation are generated in shocks associated with the jets (see (Marscher & Gear 1985) and references therein). In this model shocks propagate along the jet from denser to less dense regions. In this process, the frequency at which the perturbed region becomes optically thin decreases with time. It follows that the millimetre emission increases and the frequency of the peak emission is displaced towards lower frequencies. In the next stage, the region expands quasi adiabatically, the radiation losses being less important. Flares are thus described by a flux increase in the millimetre domain that propagates to lower frequencies with time. (See Türler et al in preparation for a 3-dimensional (flux versus time and frequency) representation of the model for average flares).

The spectral energy distribution is more complex than a single power law (Fig. 4). In many AGN the presence of broad humps as seen here at 10 GHz is taken as

evidence for the presence of cool dust at large distance from the ultraviolet source of the nucleus. Here, the large amplitude of the variability on short timescales (of the order of a year) indicates rather the superposition of several synchrotron components.

It is possible to describe the radio-millimetre flux variations up to frequencies of 100 GHz by a set of successive independent events (Türler et al., work in progress) in such a way that the resulting light curves are all well described. Each event is parametrised by a rise time and a decay, a spectrum and the time of the start of the event and its intensity. The decomposition is performed by fitting a set of flares (about 1 per year) simultaneously to more than 10 light curves covering the spectrum from 0.3 mm (1 000 GHz) to 10 cm (3 GHz) during the last 20 years. This method is able to isolate individual outbursts and to derive their evolution as a function of both time and frequency. Preliminary results show that the observed properties of a typical outburst in 3C 273 are in good qualitative agreement with the predicted properties by shock models in relativistic jet like those of (Marscher & Gear 1985).

### 3.2. Millimetre and infrared emission

Figure 5 gives the average spectrum between  $10^{11}$  Hz and  $10^{14}$  Hz extracted from Fig. 1. This continuum spectral energy distribution is characterised by a power law of index of  $0.7 \pm 0.1$  (between  $10 \mu\text{m}$  and  $100 \mu\text{m}$ ) and a "bump" around a few microns (see below).

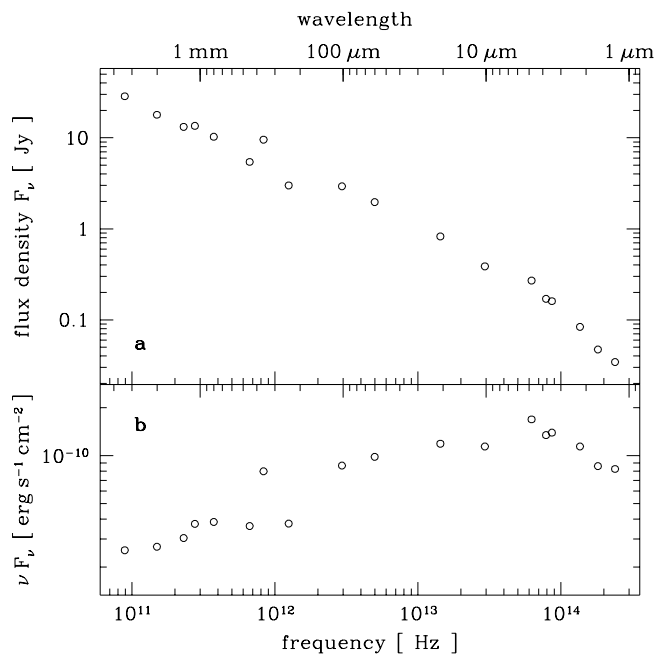


**Fig. 5.** The average millimetre-infrared spectrum of 3C 273. Data from Fig. 1. Panels as in Fig. 4.

Early infrared data are presented in (Neugebauer et al. 1979) and in (Rieke & Lebofsky 1979). (Neugebauer et al. 1979) note that the  $3 \mu\text{m}$  flux of 3C 273 and other quasars is in excess of a power law that would link the  $1 \mu\text{m}$  and the far

infrared fluxes. They suggest that this bump (easier to see in the  $\nu \cdot f_\nu$  representation) around  $3 \mu m$  may be due to the presence of heated dust, the emission of which is superimposed on the non thermal emission that extends smoothly from the radio domain. A similar conclusion is reached by (Allen 1980). The presence of dust within the nucleus might also explain the ratio of Ly $\alpha$  to H $\alpha$  fluxes which is an order of magnitude less than the theoretical predictions (Hyland et al. 1978). Dust located within the line emitting region could, according to these authors, lower this line ratio through reddening effects. Indeed, even small amounts of reddening will considerably decrease the Ly $\alpha$  flux while the H $\alpha$  flux will remain nearly unperturbed. Continuum observations suggest, however, that this dust does not redden the continuum in the same way. There is in fact no indication of substantial reddening in either the UV domain or the X-ray domain (see below) in excess to that caused within our Galaxy.

### 3.2.1. Variability of the millimetre-IR emission

The first observation of a millimetre outburst in 3C 273 is described in (Robson et al. 1983) who followed the spectral energy distribution throughout the event. This was subsequently interpreted by the model based on a shock in an expanding jet mentioned above (Marscher & Gear 1985). Although the model is probably too simplistic to be directly applicable, it remains one of the main tools to understand the radio and millimetre variability of 3C 273 and other sources.

The millimetre observations of 3C 273 in 1986 showed (Robson et al. 1986) that the sub-millimetre flux could also decrease to levels well below that normally observed. This happened while the infrared flux remained constant at wavelengths shorter than  $10 \mu m$ . The radio-millimetre emission of 3C 273 is thought to be due to synchrotron emission. Energetic synchrotron emitting electrons radiating at high frequencies lose their energy faster than less energetic electrons radiating at lower frequencies. The behaviour observed in 1986 is therefore in contradiction with expectations based on synchrotron emission. This result firmly established the presence of another component in the infrared continuum of 3C 273. The small amplitude of the variations in the near infrared and the arguments described above strongly suggest that this component is due to dust close to the sublimation temperature.

The infrared emission of 3C 273 is due to 2 very different components. On one side, the dust that has already been mentioned and on the other a rapidly flaring component that is observed only during short but violent events (see Fig. 2). This activity was observed for the first time in 1988 (Courvoisier et al. 1988). The flux variations observed then are such that, assuming isotropic emission, the luminosity changes are about  $6 \cdot 10^{40}$  ergs s $^{-2}$ . The polarization during the flare (few percent) was much larger than during quiescent periods. Both the strong variations and the high polarization imply that this flaring component is of synchrotron origin. Using the variability timescale in the K band and assuming that the emission is due to electrons cooling through synchrotron emission, (Courvoisier et al. 1988) deduced that the magnetic field was of the order of 1 Gauss and the Lorentz factor of the electrons emitting the flare of the order of  $10^4$ . It was later established that these flares may be at the origin of new components in the VLBI jet of 3C 273 (see Sect. 6.2). A similar flare probably occurred in 1990 (see Fig. 2), as can be seen in the long term light curves. It is not possible to study the duty cycle or the frequency of this activity, as the flares are very short and the flux during the flares is extremely



variable. The flares are therefore easily missed in long term sets of observations which do not have a sufficiently dense sampling to systematically catch the events.

It is interesting to note that the energy radiated during the synchrotron flare of 1988 is of the order of  $10^{51}$  ergs (an isotropic flux of 20 mJy in a band width of  $1 \mu$  in the near infrared at a distance of 1 Gpc for about 1 day) and to consider whether the radiated energy could have been stored in the magnetic field. The energy available in a magnetic field of about one Gauss as deduced in (Courvoisier et al. 1988) over a volume of a few light days across is of the order of  $10^{46}$  ergs, insufficient to explain the flare. Another possible energy source is the kinetic energy of mass ejection. Assuming a mildly relativistic velocity of  $0.1 c$  decelerated in about one day as the flare energy source one estimates that about  $6 \cdot 10^{26}$  g must be decelerated and produce synchrotron radiation with a 100 % efficiency to explain the observed luminosity variations. This is the mass accreted by the central black hole every second (see Sect. 8). These estimates would need to be modified if the radiating material was moving at relativistic velocities and emitting non-isotropically.

The millimetre activity linked to the rapid flares is also very violent. The infrared variations do not formally require that the emitting electrons have a bulk relativistic motion. The millimetre emission associated with these flares cannot, however, be understood in terms of synchrotron cooling by a static source in a constant magnetic field (Robson et al. 1993). Indeed the millimetre activity of 3C 273 is particularly complex with many flares of different characteristic times. The spectrum of individual flares and their evolution cannot, therefore, be confidently extracted.

### 3.3. The blue bump

Seyfert galaxies and quasars are generally characterized by an excess emission in the optical UV region of the spectrum when compared to the high frequency extrapolation of the infrared continuum. 3C 273 is no exception. This excess has been called the blue bump or the big blue bump to distinguish it from a smaller bump due to blended FeII lines. We will use the first name here. Figure 6 gives the average spectrum obtained in the optical and ultraviolet domains.

It has been proposed by (Shields 1978) that the blue bump might be due to thermal emission from the surface of an optically thick but geometrically thin accretion disc. The structure of these discs in which the energy released at each radius is the gravitational energy locally lost by the gas spiraling inward had been calculated by (Shakura & Sunyaev 1973). The emitted spectrum is the superposition of black bodies of temperatures decreasing from the inner radius to the outer radius of the disc. Ulrich (1981) and Malkan & Sargent (1982) fitted the observed blue bump emission with this model which they approximated by a single temperature blackbody. The temperatures they deduced from the fits were 21 000 K and 26 000 K respectively. The size of the source was estimated from the Stephan-Boltzmann law to be close to  $10^{16}$  cm using the observed flux and assuming as we do here  $H_0 = 50$  km/sMpc and isotropic emission. More detailed attempts to represent the optical-ultraviolet emission of 3C 273 using standard accretion disc models followed.

The blue bump is broader than the spectrum of a single black body. Accretion discs do have a distribution of temperatures. Fits to the data therefore improved when disc models replaced single temperature representations (Malkan 1983). The accretion disc models can be parametrized in terms of the central mass of the black hole and the accretion rate. (Malkan 1983) obtained from his fit to the 3C 273 optical and UV

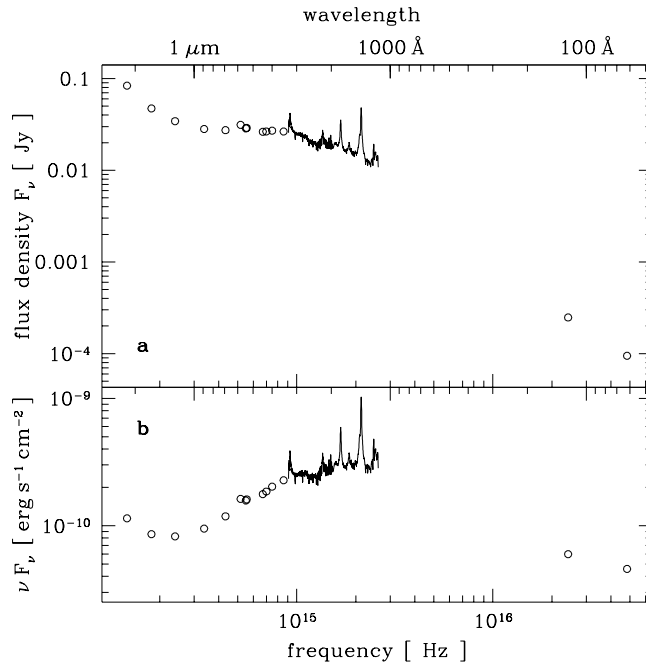


**Fig. 6.** The average optical-ultraviolet spectrum. Data from Fig. 1. Panels as in Fig. 4.

data a mass between 2 and 5  $10^8$  solar masses for the mass of the black hole and an accretion rate  $\dot{M}$  between 4 and 12 solar masses per year. The resulting ratio of the luminosity to the Eddington luminosity (the luminosity for which gravitational attraction and radiation pressure balance each other) was slightly larger than 1. It must be noted that these fits depend on the assumptions made for the underlying components. Different extrapolations of the infrared flux onto which the blue bump is added lead to different blue bump spectral energy distributions to be fitted by the models (Camenzind & Courvoisier 1984).

These early papers were followed by a large effort in which different assumptions were made to describe the components other than the disc emission (in particular the possibly underlying extrapolation of the infrared component and the free bound emission were taken into account). Meanwhile the accretion disc models grew more complete, including optically thin parts and a corona. These models can account for many features of the blue bump emission of quasars and are a natural consequence of accretion of matter with some angular momentum provided that an adequate source of viscosity is available to transport angular momentum towards the outer regions of the nucleus. (Czerny 1994) provides a review of the arguments in favour of these models.

There are, however, a number of difficulties with the accretion disc model in the case of 3C 273 and other well studied Seyfert galaxies (Courvoisier & Clavel 1991). These difficulties relate to the shape of the continuum emission, the dependence of this shape on the luminosity of the objects and the variations observed in the blue bump emission (see below).

### 3.3.1. The variability of the blue bump

There exists a very long history of observations of 3C 273 beginning in 1887. The object is indeed bright enough to be measurable on a large number of photographic plates. The data up to 1980 have been collected, homogenised and analysed by (Angione & Smith 1985). This light curve shows variations by more than one magnitude and no strictly periodical signal.

The optical-ultraviolet emission of 3C 273 varies on many timescales. One form of variation, that due to the synchrotron flares, has already been mentioned when the infrared variations were discussed. The synchrotron flares are indeed observed at higher frequencies than the near infrared into the optical domain (Courvoisier et al. 1988). Outside of the periods of intense flaring the contribution of the synchrotron emission to the blue bump is negligible. This can be deduced from the fact observed by (Robson et al. 1986) that the near infrared emission is not affected when the synchrotron flux decreases. The synchrotron power law being steeper than the blue bump spectrum will contribute less to the blue bump than to the near infrared emission. Since its contribution is not measured in the near infrared it will therefore indeed be negligible compared to the other components making the blue bump.

Ultraviolet variability of 3C 273 was first discussed by (Courvoisier & Ulrich 1985). This discussion was expanded using 9 years of IUE data in (Ulrich et al. 1988). This work showed that it is not possible to account for the changes in the continuum spectral energy distribution by a variable uniform absorbing medium. Indeed such a medium would have to alter its reddening law (hence its composition) at the different epochs at which the flux varied. Difference spectra showed that the variations are more pronounced at short wavelengths and could be accounted for by a black body of  $3\text{-}6 \cdot 10^4$  K that changes its emitting area. The recent data described below suggests more complex interpretations for the optical-ultraviolet variations.

The blue bump variability can now be well described using the 10 years of intense monitoring at optical and UV bands obtained since 1985 and shown in Figs. 1 and 3. Analysis of these data (Paltani 1995) and (Paltani et al. 1998) in terms of a structure function shows that the longest timescale on which the source varies is slightly shorter than a year at the shortest wavelengths available with IUE ( $1200 \text{ \AA}$ ) and longer than 3 years (i.e. longer than a third of the available timespan of controlled photometric observations) in the V band.

A cross correlation analysis of the light curves shows, furthermore, that all the light curves are very well correlated at short lags (less than a month, see below) but that a secondary correlation peak monotonically increases when longer wavelength light curves are correlated with the  $1200 \text{ \AA}$  light curve.

Both of the above observations indicate that the blue bump variations are of a complex nature and cannot be due to a single physical component. Indeed, a single component like a black body of variable emitting area, is expected to show the same variation timescales at different wavelengths. (Paltani & Walter 1996) have proposed a decomposition into two components for a set of AGN including 3C 273 based on the suggestion that one component is stable or at least varies on timescales much longer than the other and that the spectral energy distributions of both remain stable, the variability being due to the changes of the relative normalisation. This decomposition has the interesting side benefit of giving a very high signal to noise spectrum that allows the measurement of the reddening, in the case of 3C 273  $E_{B-V} = 0.038$ , compatible with galactic reddening.

At very short lags, the lag of the peak of the cross correlation between the 1200 Å light curve with those at longer wavelengths increases with wavelength. The lag is of 2 days at 2000 Å and 10 days for the V band (Paltani et al. 1998). These lags, although probably significantly different from zero (note that it is difficult to give a formal uncertainty on the lag at which a cross correlation peaks) is many orders of magnitudes less than that expected from viscously heated accretion disc models (Courvoisier & Clavel 1991). This result is insensitive to the details of the models and is also valid for other temperature distributions than those of standard accretion discs. In particular the lag is much shorter than the sound travel time in the accretion disc between the hot regions emitting the UV flux and the cooler regions emitting the V band flux. The lag between the UV and optical light curves of a few days implies that if an accretion disc is present it must be heated by an external source rather than by the internal dissipation of gravitational energy in an optically thick medium. More generally, this result states that the causal connection between the hot and cool regions that form the blue bump (i.e. those emitting in the ultraviolet and those emitting in the visible) must be based on information transported at speeds close to that of light. This observation is similar to that obtained for those Seyfert galaxies for which adequate data have been obtained.

The fact that the energy source should be located outside the disc has several implications. First the standard disc structure and spectra as deduced using the local gravitational energy dissipation (Shakura & Sunyaev 1973) is not applicable, secondly the origin of the heating source must be sought. In other words, one should find a way of radiating the energy freed by the accretion process outside the disc.

One possibility that has been studied is the presence of hot coronae surrounding the discs (Haardt et al. 1994). In this paper Haardt et al. consider a structured corona in which a fraction of the accretion power is released through magnetic interactions. The hot blobs in the corona reprocess a fraction of the disc soft photons to X-rays.

### 3.4. X and gamma-ray emission

(Bowyer et al. 1970) have reported the first convincing evidence for X-ray emission from 3C 273 using a collimator instrument on a sounding rocket. This result was confirmed by Uhuru measurements reported by (Kellogg et al. 1971). In a 1977 review (Gursky & Schwartz 1977) state that 3C 273 is still the only quasar reliably associated with an X-ray source and that it is not certain that X-ray emission is a characteristic of active galactic nuclei in general. This has changed since then, X-ray emission is one of the important emission components of all classes of AGN. 3C 273 has thus been observed, often many times, by all X-ray satellites. We present here the X-ray data to about 10 keV obtained by EINSTEIN (Wilkes & Elvis 1987), EXOSAT, GINGA (both reported in (Turner et al. 1990)), ROSAT (Leach McHardy & Papadakis 1995) and (Walter et al. 1994), ASCA (Yaqoob et al. 1994) and SAX (Grandi et al. 1997) and higher energy data as discussed in (Maisack et al. 1992) for HEXE data, (Bassani et al. 1992) for SIGMA data and (McNaron-Brown et al. 1995) for OSSE data.

This emission has 4 features (see Fig. 7): A steep low energy component that emerges from the interstellar absorption called the soft excess, a straight power law that extends to about 1MeV (which we will call the medium energy component) on which a weak Fe line appears and a steeper power law above about 1 MeV (called the high energy component in the following).

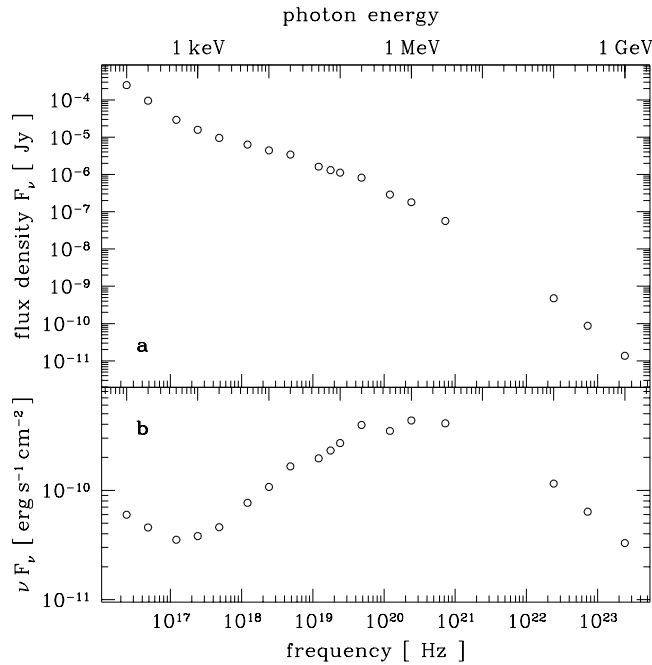


Fig. 7. The average X and gamma-ray spectrum. Data from Fig. 1. Panels as in Fig. 4.

### 3.4.1. The soft excess

Low energy X-ray data on many AGN cannot be fitted by extrapolation of the power law that is used to describe the medium energy component. The flux observed at low energies ( $\lesssim 0.5$  keV) is systematically larger than that predicted by this extrapolation. Since the presence of cold matter along the line of sight decreases the low energy X-ray flux we can deduce that there are no large amounts of cold material in excess of that within our Galaxy. The soft excess (common also in Seyfert galaxies) is poorly characterized as it extends into the low energy region in which the flux is completely absorbed by interstellar matter, because only few energy resolution elements are available (this is expected to change with the launch of the XMM satellite in 1999) and because the amount of absorbing matter on the line of sight is not known. One way of fitting the data is by an optically thin thermal emission model of  $k \cdot T \simeq 0.2$  keV, another is to use a power law of photon index  $-2.7$  (Leach McHardy & Papadakis 1995). These fits should be taken as a mathematical description of the shape of the emission rather than as a true physical description of the emission.

Simultaneous observations in the UV and X-ray domains in a set of objects including 3C 273 (Walter et al. 1994) and (Walter & Fink 1993) indicate that the parameters of the soft excess and those of the blue bump are correlated. Should this be confirmed, it would show that the soft excess is the high energy tail of the blue bump. This high energy end of the blue bump would then occur at roughly the same energy for nuclei of very different luminosities, a fact unexpected in standard accretion disc models in which the maximum temperature is expected to decrease with the  $1/4$  power of the luminosity (Courvoisier & Clavel 1991).

### 3.4.2. The medium energy component

At energies higher than about 0.5 keV, the spectrum is well described by a single power law extending to the MeV region. There is no hint of any curvature in this spectrum, contrary to predictions of models in which the X-ray flux is in part reflected by the surface of a cool disc. These latter models predict the presence of a so-called reflection hump corresponding to the Compton reflection of the primary component. This hump is observed in many Seyfert galaxies (Mushotzky Done & Pounds 1993), but not in 3C 273 (Maisack et al. 1992), (Grandi et al. 1997). This result is surprising because 3C 273 has a bright blue bump. Indeed, reprocessing models (models in which the blue bump emission is due to a disc heated by an external X-ray source) predict that an important blue bump would be linked to the presence of re-processing signatures also in the X-ray domain.

The spectral slope of this component is typically 0.5 and shows evidence for some variations (see below). As a result, the energy radiated per logarithmic energy interval ( $\nu \cdot f_\nu$ ) peaks at the energy at which the spectral break is observed, i.e. around 1 MeV.

### 3.4.3. The Fe line

A further signature of X-ray reprocessing by cold material is the presence of a fluorescence emission line at 6.4 keV. There is some evidence for the presence of a weak line at this energy in the X-ray spectrum of 3C 273. One of the GINGA observations (in July 1987) showed evidence for the line at the 99% confidence level. The line equivalent width was 50 eV, the corresponding line flux was  $4.5 \pm 2.5 \cdot 10^{-5}$  photons  $\text{cm}^{-2} \text{s}^{-1}$  (Turner et al. 1990). The other GINGA observations reported by (Turner et al. 1990) provided only upper limits to the line flux compatible with the one of July 1987. Since the continuum flux had varied significantly this means that the line equivalent width did vary. A further line detection is reported by (Grandi et al. 1997) in a SAX observation in July 1996. The equivalent width was  $30 \pm 12$  eV. Other observations, by EXOSAT and ASCA provided only upper limits (Turner et al. 1990) and (Yaqoob et al. 1994). This somewhat confused set of measurements probably means that there is a weak line present in the emission of the quasar but that the data available do not allow us to perform a convincing analysis of the line variability nor of its relationship with the continuum variations. This study will be of prime importance to understand where the cold matter emitting the fluorescence line is located with respect to the primary X-ray source.

### 3.4.4. The high energy component

Early gamma ray detections were due to the Cos-B satellite. The source was identified in the data from the position coincidence of a compact source (i.e. a source not resolved by Cos-B) with the position of the quasar (Swanenburg et al. 1978), (Bignami et al. 1981).

The flux above a few MeV is well described by a power law of index  $1.4 \pm 0.1$  (Lichti et al. 1995). This index has been shown to vary between  $1.2 \pm 0.2$  and  $2.2 \pm 0.5$  (von Montigny et al. 1997), hardening with increasing flux (we give here energy spectral indices rather than photon indices to remain consequent with the discussion of the spectrum at lower energies). Quite expectedly, the spectral index around 1 MeV

is between the X-ray spectral index and the one observed at higher energies as it is in this region that the spectrum steepens from a slope of about 0.5 to one of 1.5. It must be stressed that the high energy component described here is a power law and not an exponential cut-off of the medium energy component. This spectral break is an important constraint to any model, it is larger than 0.5, the value expected from simple one component Compton cooling models. Models for the high gamma-ray emission of beamed AGN include the relativistic electron positron beam model of (Marcowith et al. 1995). In this model the emerging emission is due to inverse Compton process of relativistic electron position pairs on the soft photons from the accretion disc. The observed spectral break is due to the energy dependence of the gamma-ray photosphere defined by the optical depth to pair production being equal to one. A further model is suggested by (Mannheim 1994) and (Mannheim 1993) in which ultra relativistic protons generate gamma ray photons via pion and pair photo production.

Several candidate models have been fitted to the data by (Lichti et al. 1995) and (von Montigny et al. 1997). They are all based on the assumption that the gamma ray component is emitted by electrons or/and hadrons in the relativistic jet. This assumption is due to the remark that the high energy photon density estimated from the observed flux and the time scale of variability implies that the electron-positron pair production optical depth is considerably larger than one. This would imply that the high energy photons cannot escape from the source region. This is formally described by the dimensionless compactness parameter  $l$ :

$$l = \frac{\sigma \cdot L}{mc^3 \cdot R},$$

where  $\sigma$  is the pair production cross section,  $L$  the luminosity and  $R$  the size of the source as deduced from the source variability timescale. Using  $\sigma \simeq \sigma_{Thompson}$ , a variability time scale of 0.5 days as given by the Ariel V measurement described below and a maximum observed gamma ray luminosity, (Lichti et al. 1995) deduce a compactness of 210, implying that the optical depth of the region to pair production ( $= l/4\pi$ ) is much larger than 1. Using a more established variability time scale for the medium energy component of several days does relieve the compactness question and lessen the justification for identifying the high energy emission of 3C 273 with the relativistic jet. It should be noted, however, that in other sources, the BL Lacs observed at very high energy, the compactness is such that the gamma ray emission must be emitted by strongly relativistic jets, justifying a similar assumption also in the case of 3C 273.

#### 3.4.5. X-ray variability

The X-ray flux of 3C 273 varies considerably. The first report of this variability is by (Marshall et al. 1981) who detected an 80% flux increase in a 40 000s Ariel V observation. This is the only report of very strong and short flux variation in 3C 273. Since Ariel V was not an imaging instrument, there is a possibility of source confusion. This result is therefore in strong need of confirmation by an imaging instrument.

The flux of the soft excess has been found (Courvoisier et al. 1987) to be variable in time and to vary independently of the medium energy component. (Courvoisier et al. 1990) reported a variability of 4% in about 17 hours in the medium

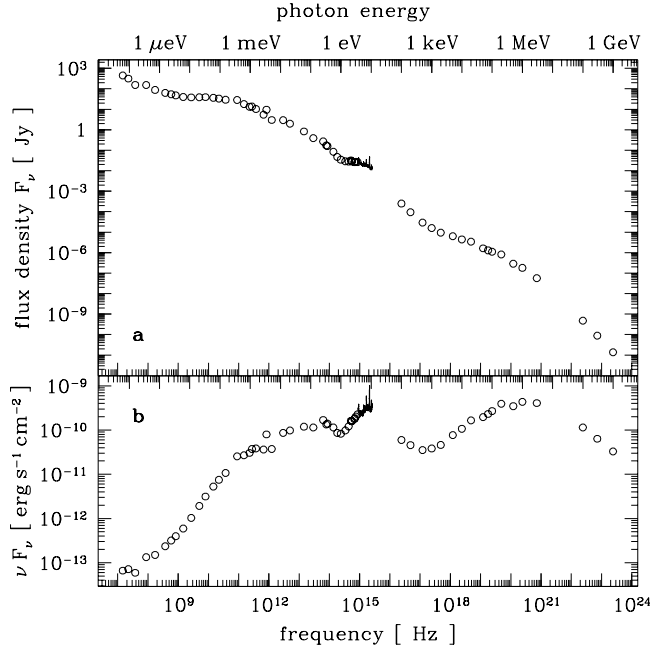


**Fig. 8.** Overall average spectrum of 3C 273 (first panel). This corresponds to a projection onto the frequency axis of all data in Fig. 1. The bottom panel shows the same data as above but represented as  $\nu \cdot f_\nu$  versus  $\nu$ .

energy component observed by EXOSAT. (Leach McHardy & Papadakis 1995) analysed 14 ROSAT observations. They confirm that the soft and medium energy X-ray components vary independently and reported their fastest variations to be by about 20% in 2 days in the soft energy band (0.1-2.4 keV) observed by ROSAT.

The 2-10 keV flux observed by EXOSAT and GINGA indicate variations from  $0.60 \cdot 10^{-10}$  to  $1.68 \cdot 10^{-10}$  ergs  $\text{cm}^{-2}$   $\text{s}^{-1}$  for the medium energy component. This was obtained with 13 observations spanning about 5 years. The resulting light curve is hopelessly undersampled, preventing any description of the flux variations.

This data set also provided evidence that the spectral slope in the same energy domain varies by small but significant amounts. The spectral slope is not correlated with the flux but is anti-correlated with the logarithm of the 2-10 keV count rate divided by the UV photon rate (Walter & Courvoisier 1992). This result is interpreted in this paper as being the signature that the medium energy X-ray component is due to a thermal Comptonisation process of the UV photons by an electron population of about 1 MeV covering a few percent of the UV source with an optical depth of 10-20%. Work in progress shows that when using the BATSE data as displayed in Fig. 2 one finds a weaker anti-correlation between the spectral slope. This work should, however, take into account the delay between the UV and the X-ray light curves. This delay (discussed below) indicates that the UV flux Comptonised in the hot regions may not be that observed simultaneously, but rather the UV flux observed about 2 years earlier. This may not have had much effect in the early phases of the monitoring because the UV flux was relatively quiet compared with later epochs.



### 3.5. The Overall continuum spectral energy distribution

Having studied the emission components separately we can now put all these elements together. To do so we present in Fig. 8 the average spectrum obtained by projecting all the data of Fig. 1 onto the frequency axis. Figure 8 also gives the same data but in the form of  $\nu \cdot f_\nu$  versus  $\nu$ . It is striking that the flux per logarithmic interval is nearly constant over more than ten decades of frequency, another way of expressing that to the first order the emission is proportional to  $\nu^{-1}$ . In the second order, it is striking to see two maxima in the  $\nu \cdot f_\nu$  versus  $\nu$  distribution at roughly the same level, one in the far ultraviolet and the other at about 1 MeV.

Integrating the spectrum one can deduce the total flux in the average spectrum and the bolometric luminosity of 3C 273. One finds a total flux of  $1.9 \cdot 10^{-9}$  ergs  $\text{s}^{-1} \text{cm}^{-2}$  and assuming isotropic emission,  $H_0 = 50 \text{ km}/(\text{s Mpc})$ ,  $\Omega = 1$  and  $q_0 = 0.5$  one finds a luminosity of  $2.2 \cdot 10^{47}$  ergs  $\text{s}^{-1}$  (Türler et al. 1998).

## 4. The multi-wavelength approach to the continuum emission

Studying each component or equivalently the observations in individual spectral domains provides information on the physical processes at the origin of the components. It does not, however, provide a full picture in which it is possible to see how the gravitational energy released by accretion is distributed between the various cooling channels, nor does it allow us to describe the respective geometrical arrangements of the components or their physical relationships. Correlated studies across the complete electromagnetic spectrum are necessary for this research. 3C 273 is a prime source for these studies as it is bright in all bands and located close to the celestial equator. Both characteristics provide for ease of access with many instruments.

An early and surprising result was obtained by (Courvoisier et al. 1990) who showed that the UV light curve leads the radio emission by a few months. This result is confirmed by continued monitoring (Courvoisier 1997) and may be understood if the blue band flux is a signature of the accretion process (and hence of the energy release) and the radio (synchrotron) emission one of the cooling channels located at some distance from the central black hole. In this case and assuming that part of the accretion energy is carried along the VLBI jet (described in Sect. 6.2) and with its velocity from the central source to the location of the radio emission, the observed delay of approximately 0.4 year can be used to estimate the distance  $D$  at which the radio (22 GHz) flux is emitted:

$$D = c \cdot \Delta t \cdot \left( \frac{1}{\beta_j} - \cos \theta_j \right)^{-1},$$

where  $\beta_j = 0.95$  is the VLBI jet velocity divided by  $c$  and  $\cos \theta_j = 0.95$  the cosine of the jet angle with respect to the line of sight (Davis Unwin & Muxlow 1991). These data imply that the radio emission is located some 4 light years from the central source along the jet.

(Clements et al 1995) have also performed a correlation analysis of the blue bump and radio light curves. They used photographic photometry from the Rosemarie Hill observatory taken from 1974 to 1992, radio data from the University of Michigan Radio Astronomy Observatory and data from the Algonquin Radio Observatory from 1966 to 1990. Cross correlating the optical and radio light curves does not provide a significant signal at any lag. This stems most probably from three factors. The blue

bump light curve is undersampled and was obtained from B band observations rather than ultraviolet. Furthermore the radio light curve is at 10 GHz, less than that used in the preceding analysis. At lower radio frequencies, the light curves are smoother and the amplitude of the variations decreases (Teräsraanta et al. 1992). This effect probably smoothes the variations in 3C 273 to the point at which the correlation with the optical variations is lost. It is interesting to note, however, that (Clements et al 1995) and (Tornikoski et al. 1994) do find significant correlations between the radio and the optical light curves in several other objects. The optical light curves always lead the radio light curves. Typical lags are of the order of several months similar to those obtained in the case of 3C 273.

Using the radio and ultraviolet data, one may also wonder whether it is possible that 3C 273 is a mis-directed BL Lac object. Indeed 3C 273 has a strong synchrotron source emitting in the radio and millimetre domain and a superluminal jet. Both are characteristic of BL Lac objects. Were the blue bump and the emission lines overwhelmed by the synchrotron emission, one might well classify 3C 273 as a BL Lac type object. For this to be the case, the synchrotron component should, however, be boosted by a factor larger than  $10^3$  (Courvoisier 1988). The resulting radio flux would then be larger than  $3 \cdot 10^4$  Jy, a highly improbable flux. It would thus appear that the presence of a strong blue bump and bright emission lines is an intrinsic difference between BL Lac objects and quasars like 3C 273 rather than due to orientation effects.

The relation of the UV with the X-ray emission is of considerable interest to test reprocessing models. One aspect of this correlation has already been discussed when the slope of the X-ray component was compared to the ratio of X-ray to UV photons. Cross correlating the IUE and BATSE light curves, one finds a very significant correlation peak at a lag indicating that the X-ray light curve follows the UV light curve by 1.75 years and no significant correlation close to zero lag (Paltani et al. 1998). Assuming that this result represents a physical reality rather than a chance occurrence of features in the light curves, (Paltani et al. 1998) conclude that the Comptonising X-ray emitting medium could be heated in a shocked region formed in a mildly relativistic wind at about 1 pc from the central source, in good agreement with the model proposed by (Courvoisier & Camenzind 1989) and described in Sect. 8. It is, however, also possible to apply models in which the Comptonising medium is located on the surface of the soft photon source (e.g. on the surface of an accretion disc). In this case, the flux correlation cannot have a physical meaning and, provided that the temperature of the plasma is known (e.g. from (Walter & Courvoisier 1992)), one deduces an X-ray spectral slope as a function of time assuming a variable optical depth in reasonable agreement with the existing data.

Looking at the correlations between the X-ray and the radio light curves, one finds no significant correlation at zero lag (Courvoisier et al. 1990), (Courvoisier 1998). This indicates that the X-rays cannot be due to a simple synchrotron self-Compton process in which the radio photons are scattered by the same electron population that produced them in the first place. The light curves now available indicate that the medium energy X-ray and radio components are correlated when the X-rays emission follows the radio by 2.2 years. This result is however, based on a dominant flare in the X-ray light curve, it remains then to be seen whether it proves solid with time.

Taken at face value the data presently available indicate that the UV flux leads all the other components. The typical delays are of the order of one or very few years. This result is in strong need of confirmation. It will, however, take many years of careful multi-wavelength observations to do so. This result would considerably strengthen the conjecture that the UV emission is a signature of the accretion and

that the released energy is transported from the central regions of the gravitational potential well to the regions where it is radiated by relativistic or near relativistic flows.

## 5. Line emission

Line emission is one of the defining properties of quasars. It has also been one of the main lines of research over the last three decades. The information content of the spectrum is -trivially- richer in the lines than in the continuum. Unfortunately, the information gained from the emission line does not allow researchers to gain much understanding on the mechanisms at the origin of the radiation. This must be obtained out of the relatively information poor continuum. What the information provided by the lines allows us to do is to describe the gas surrounding the energy source. This includes a description of the physical state of the gas (temperature, density, ionization level), of its kinematics through the width of lines and of its geometrical arrangement (filling factor) through the equivalent width of the lines. A general review of these inferences can be found in (Peterson 1997) and (Netzer 1990). A detailed fit to all line features in 3C 273 can be found in (Wills Netzer & Wills 1985).

The classical picture is that the lines are formed in a set of photoionized "clouds" in rapid movement around the central black hole. The smoothness of the lines implies that the number of clouds must be large. How large is however not known yet (see Dietrich et al. in preparation). The continuum at the origin of the photoionization is normally associated with the central source.

Whereas one would expect that the study of the line intensity ratios should be able to provide a description of the ionizing continuum (since the lines come from elements that have different ionizing potentials) particularly in the unobservable part of the spectrum between 912 Å and ~0.1 keV few concrete results have emerged (Binette et al. 1988), (Krolik et al. 1988).

(Wills Netzer & Wills 1985) claim that the photoionization models they use represent well all the line features of the quasars they describe with the notable exception of the FeII line blends observed in the optical and UV parts of the spectrum. 3C 273 is no exception to this "FeII problem". Expected values for the intensity ratios of FeII lines to Ly $\alpha$  is of 0.3-0.5 (Netzer 1990) whereas the observed ratio (corrected for a reddening  $A_V = 0.16$  corresponding to the galactic reddening  $E_{(B-V)} = 0.05$  as used in (Ulrich et al. 1988)) is slightly larger than 1 (Wills Netzer & Wills 1985). Clearly, assuming a more important intrinsic reddening will tilt the FeII lines to Ly $\alpha$  ratio to smaller values, lessening the problem; there is, however no reason to assume a large intrinsic reddening (see above). This problem is as of yet unsolved and may point to additional energy sources in the broad line clouds (e.g. mechanical heating) and/or to a more complex structure of the broad line region than envisaged in most photoionization calculations (Collin-Souffrin & Lasota 1988).

Whatever the details of the fits and the agreement of the line intensities with various photoionization models, a very important point is that the heavy element abundances are large, in some instances larger than solar. This indicates that the gas surrounding quasars, and in particular 3C 273, has been going through one or several generations of star formation and explosion before being found in the very inner regions of the galaxies hosting the quasar.

### 5.1. Line variability

Some carefully designed observation campaigns using the IUE satellite and additional ground based data have shown that the emission line variations in Seyfert galaxies follow those of the continuum. The lag is short and increases as the level of ionization decreases. The amplitude of the variations in the high ionization lines and in particular of  $\text{Ly}\alpha$  are similar to those of the continuum. See (Peterson 1993) and references therein for a review of these results. This is one of the strongest arguments demonstrating that the emission lines are indeed due to photoionization of gas close to the continuum source.

In 3C 273, the picture is quite different. Whereas the UV continuum varies by a factor of about 2 (see above), the amplitude of the  $\text{Ly}\alpha$  variations is only 15% or less (Ulrich, Courvoisier & Wamsteker 1993), (Ulrich et al. 1988), (O'Brien et al. 1989). (O'Brien et al. 1989) studied the timescale of the  $\text{Ly}\alpha$  variations and the possible  $\text{Ly}\alpha$  continuum correlations. They claimed that the observed timescales are less than one year and that there is some correlation between line and continuum variations. The existence of such correlations and the measurement of any lag between continuum and line light curves using variations as small as those observed in 3C 273 are, however, barely possible based on the IUE data base (Ulrich, Courvoisier & Wamsteker 1993). The small amplitude of the line variations compared with the continuum variations is confirmed by a study of the IUE data on 3C 273 up to 1991 by (Türler & Courvoisier 1997) which shows that when performing a principal component analysis of the spectra of 3C 273, the principal component does not show a line, but only the continuum. This analysis, contrary to previous ones considered all the spectra of a single object as the matrix in which the principal component is to be sought. The principal component then gives for the given object the most variable "spectrum". The result obtained for 3C 273 is in contrast with other well studied objects for which the principal component has the same shape as the average broad line. In the case of 3C 273 the principal component is essentially flat, indicating that the continuum varies, not the lines. This is possibly due to the fact that in 3C 273, an intrinsically bright object, the broad line region is further from the central source than the characteristic time of the continuum variations (of the order of a year) times the velocity of light.

## 6. The jet

There are two very different aspects to the jet in 3C 273. One is the small scale jet observed with VLBI techniques and showing superluminal motions. The other is the long jet visible at radio, optical and X-ray photon energies from  $12''$  to  $22''$  from the core at a position angle of  $222^\circ$ .

### 6.1. The radio-optical jet

It was already clear at the time of the identification of 3C 273 with an optical object that the radio source had two components called A and B (Hazard MacKey & Shimmins 1963) and that the optical counterpart was coincident with the B component. The optical counterpart had some luminosity in the form of a jet extending in the direction of the A component and ending precisely at its position, (Schmidt 1963). This established from the earliest time that 3C 273 has a one-sided jet. No counterjet has ever been discovered either at radio or at optical wavelengths.

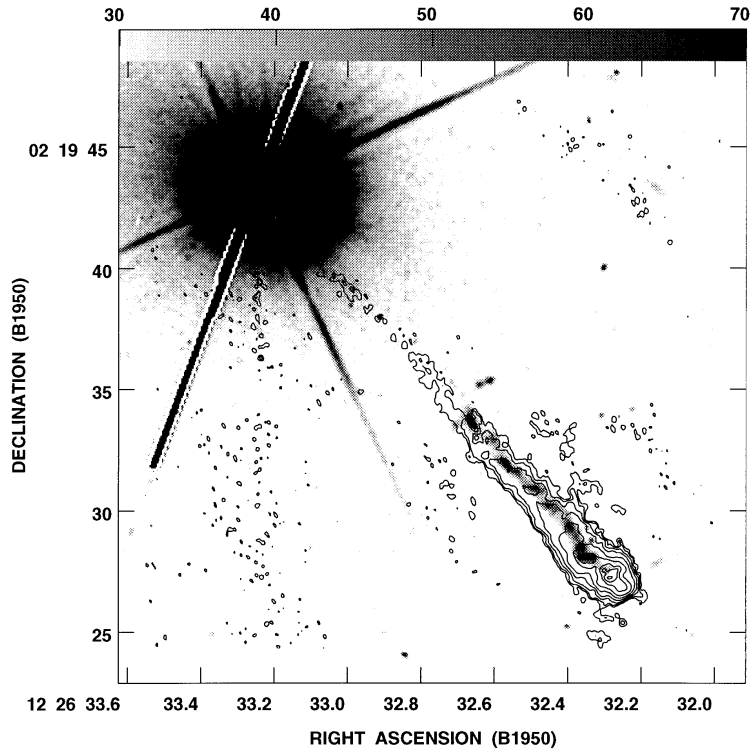


**Fig. 9.** The core and jet of 3C 273 as observed in the radio domain (contours) and with HST (grey scale). This shows that while the radio jet can be followed all the way to the core, the optical jet can only be detected in the outer regions of the jet. This figure is from (Bahcall et al. 1995).

Modern MERLIN and VLA maps and polarization have been presented in (Conway et al. 1993). At radio frequencies, the jet flux increases monotonically from the inner radius to a peak located at roughly  $21''$  from the core and then falls steeply. The behaviour is very similar for wavelengths between 2 cm and 73 cm. The polarization at 6 cm is such that the B-field is parallel to the jet axis except at the point of maximum flux (the so called hot spot) where it is perpendicular to the jet axis. At other wavelengths the polarization is qualitatively similar. The maximum polarization is approximately 20% with three spots along the ridge at  $14''$ ,  $17.5''$  and  $20.3''$  from the core where the level of polarization is very low.

The optical jet is more structured than the radio jet, it is a succession of bright spots and regions of weaker emission. Most modern work on the jet uses a simple denomination for the hot spots given by (Lelièvre et al. 1984). The spot nearest to the core is labeled A, the subsequent spots are B, C and D. Subsequent work at higher angular resolution then subdivides the spots in sub-units. Figures 9 and 10 give an optical image of the jet and labels the main spots.

Recent optical data on the jet of 3C 273 and a detailed comparison with the radio morphology and polarization of the jet are presented in (Roeser & Meisenheimer 1991), (Roeser et al. 1996a), (Bahcall et al. 1995) and in (Roeser et al. 1997). It results from these studies that the position angle of the jet as observed in the radio

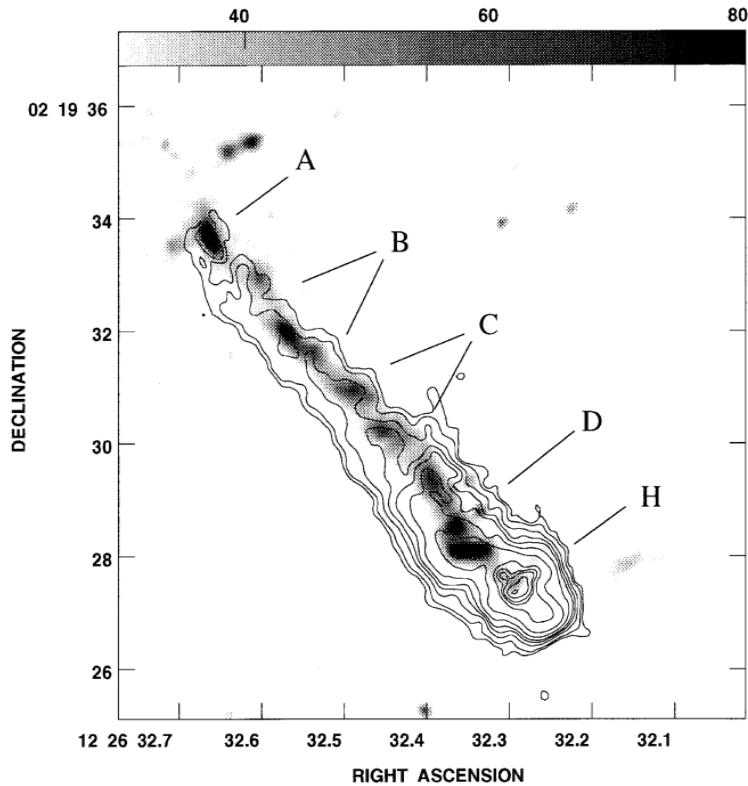


**Fig. 10.** Same data but showing an enlargement of the jet and the nomenclature of (Lelièvre et al. 1984). This figure is from (Bahcall et al. 1995).

and optical domains is the same at  $222.2^\circ$ . The general appearance of the jet in the 2 spectral domains is similar at first sight. There are, however, some notable differences. The radio jet can be followed from the core of the quasar to the brightest regions, whereas the optical jet can only be observed from some distance to the core onward. This statement is, however, clearly of limited value as it results from systematic observation limitations in detecting weak surface brightness features close to a bright point source. It is nonetheless clear that the ratio of optical to radio flux changes with distance to the core. The high resolution of the HST images reveal that the optical jet is structured on smaller scales than the radio jet and that it is narrower. The optical images show two "extensions" outside the jet axis at the inner and outer edges. At least the outer extension seems to be due to the presence of a spiral galaxy on the line of sight (Roeser et al. 1997).

The radio and optical data may be combined to obtain spectral energy distributions for the knots of the jet. The innermost knot (A) has a straight power law continuum without any sign of a cut-off in the visible or UV, whereas the subsequent knots are well described by a power law extending from 100 MHz to  $10^{14}$  Hz followed by an exponential cut-off.

The optical and radio polarization of the jet are also similar in their main properties and also show some discrepancies when looked at in greater details. The maximum

polarization is in both cases of the order of 10%, low in the inner regions ( $< 15''$ ) and rising towards the hot spot.

Spectral energy distributions and the relatively high degree of polarization both suggest that the jet emission is due to synchrotron processes. Synchrotron cooling of electrons depends on the inverse square root of the frequency. Optically emitting electrons are therefore expected to be associated with the recent history of the electron acceleration, while radio emitting electrons remember a history thousand times longer. It is thus not necessarily expected that the radio and optical jets should be similar in the location of the hot spots. It should be noted, however, that the presence of bulk relativistic motions would tend to enhance for any observer the emission of those parts of a jet that move in directions close to the line of sight. Such relativistic effects are independent of the frequency and would lead to the presence of coincident bright spots in both the radio and optical images. (Bahcall et al. 1995) suggest one model along these lines in which the jet structure would be due to a helical bulk motion of the emitting electrons within the jet.

Radio profiles of the jet perpendicular to the jet axis (Roeser et al. 1996a) show that the jet is symmetric at large distances from the core, whereas it is more extended in the South closer to the core (at  $15''$ ). This extension is not observed in the optical domain and has a steep spectral index. It is suggested that this is emission from material that has passed through the terminal shock and flows backwards along the jet.

Extended X-ray emission in the vicinity of 3C 273 has been detected with the EINSTEIN satellite (Willingale 1981). It was found that there is an excess emission in the approximate direction of the jet at distances from the core of the quasar that are compatible with the position of the radio and optical jet. The main difficulty associated with these data is that the angular distance of the X-ray excess falls well within the EINSTEIN point spread function. The data were re-analysed by (Harris & Stern 1987) who deduced a position for the centroid of the excess at  $16''$ . At this position and with the flux they deduced it was difficult to interpret the origin of the X-ray flux in terms of synchrotron, inverse Compton or thermal emission.

(Roeser et al. 1996b) report on a long (17.2 ksec) ROSAT HRI observation of 3C 273 in 1992 to which another 68.2 ksec obtained in very early 1995 were added. These authors used the emission from the core of 3C 273 to center the point spread function every 50 s and were thus able to correct for the wobble of the spacecraft. This led to a point spread function of  $4.5''$ . Two extended features can be observed in the resulting X-ray image. One is at position angle  $71^\circ$  and is assumed to be from a weak X-ray source not associated with 3C 273 while the other is at position angle  $219.3^\circ$ , close to that observed in the other wave bands. The main contribution comes from a distance to the core of  $15''$ , similar to what had been obtained with EINSTEIN. The flux derived from the ROSAT observation is, however, considerably less than that derived from the EINSTEIN data.

It was noted above that the A knot is very blue and showed no evidence of a cutoff at high frequencies. Should the X-ray emission be indeed associated with this knot, then the flux would lie on the extrapolation of the radio-optical spectral energy distribution. The position of the X-ray excess is, however, such that it does not coincide with knot A (nor with any of the sub-knots derived at high angular resolution). The next knot (B) has a spectrum that shows a clear cut-off in the optical spectrum and is therefore unlikely to extend to the X-ray domain. The difficulties in the interpretation raised by (Harris & Stern 1987) remain therefore. Were the X-rays

due to inverse Compton processes, one would like to understand why this is observed only at this location rather than associated with all the knots.

The extended jet of 3C 273 is still not completely understood. It is also noteworthy that this is the only jet from a quasar from which optical and X-ray emission have been detected to date. Optical emission from the jets of extra-galactic radio sources is a rare phenomenon, it is therefore not surprising that no other quasar jet has been observed at higher frequencies than the radio domain. It will nonetheless make the task of understanding the nature of the extended jet of quasars very difficult.

### 6.2. *The VLBI jet*

The core of 3C 273 (3C 273 B as it was called in the 1960s) is a very bright radio source. The presence of the jet described above at large angular distances showed that the source is not point like, but has an interesting geometry. Both facts made 3C 273 a prime source for high resolution radio observations as these became possible by using together telescopes spanning approximately the size of the Earth (Very Long Baseline Interferometry, VLBI in short). Early observations used few telescopes and did not produce maps but were able to measure whether or not the source is extended at certain angular scales. (Brotten et al. 1967) and (Clark et al. 1967) showed thus that 3C 273B has an angular size less than  $0.005''$  at a wavelength of 18cm. Structure on the scale of milli arcseconds (mas in the following) has been found by (Knight et al. 1971) and (Cohen et al. 1971) who also note a difference between their results that can be interpreted by a change in angular size of the source. Radio data (visibility functions rather than maps) confirmed the reality of the changes and revealed a steady expansion of the source between 1970 and 1977 (Cohen et al. 1977). Study of the location of the minima in the visibility curves showed an apparent expansion velocity of  $5.2c$  ( $H_0 = 55 \text{ km}/(\text{s} \cdot \text{Mpc})$ ) (Cohen et al. 1979). Maps were also obtained then, showing for the first time a real jet structure at a position angle of  $-117^\circ$ , not aligned with the larger scale jet described above (Readhead et al. 1979). Subsequent maps at higher angular resolutions and using more antennae than previously, thus improving the image quality, showed that the local maximum of the jet moves away from the core. The distance from the core to the main jet feature had increased from 6 mas in 1977.5 to 8 mas in 1980.5 (Pearson et al. 1981) corresponding to an apparent expansion velocity of  $9.6 \pm 0.5c$  ( $H_0 = 55 \text{ km}/(\text{s} \cdot \text{Mpc})$ ).

More recent VLBI observations have continued the work done at cm wavelengths, have used higher frequency observations to increase the angular resolution and have improved on the dynamical range to study weaker features. These modern data have confirmed the picture described above and added several new features.

A set of several VLBI observations in the 1980s has revealed that new jet components (often called blobs) appear every few years. These components can be followed from one observation to the next and their projected trajectories mapped. It is thus possible to trace back each component to the time of zero separation from the core (Krichbaum et al. 1990). One of the component was observed to be thus "born" shortly after a violent synchrotron outburst that had been observed at wavelengths as short as the visible band in March 1988 (see above; (Courvoisier et al. 1988)). This close association suggests that in general new components in the jet follow synchrotron outbursts. This is indeed claimed in a study of (Abraham et al. 1996) in which the ejection time of 8 components is computed and qualitatively compared to single dish light curves. We show in Fig. 11 the high frequency radio light curves and



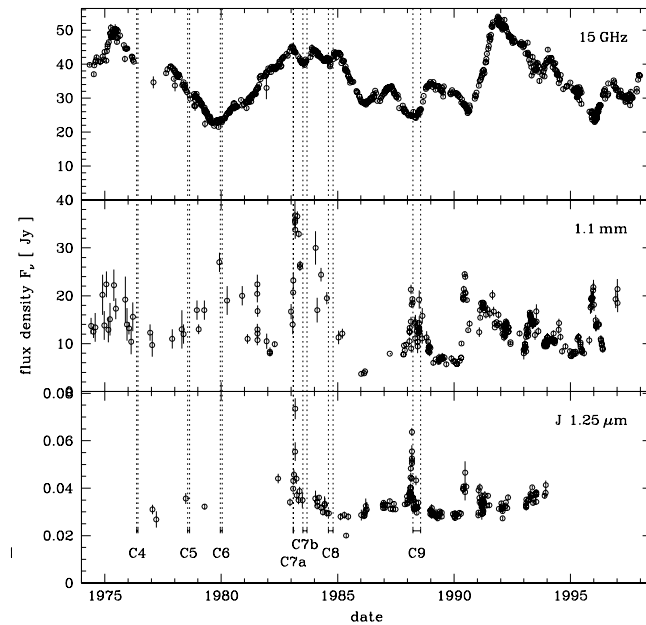


**Fig. 11.** millimetre and infrared light curves and dates of appearance of new VLBI jet components (see the text). The components are labeled as in (Abraham et al. 1996). The epochs of ejection of the components are from (Abraham et al. 1996). The uncertainty in the ejection epochs are shown by a short range.

a near infrared light curve available to us (see above) and the epochs of appearance of new jet components as computed by (Abraham et al. 1996). Whereas it seems clear that the ejection of C9 is associated with the infrared outburst discussed above, no clear statement can be made for the preceding ejections.

(Abraham et al. 1996) have also correlated the epoch of ejection of components with the radio light curve at 22 GHz they claim that the ejection times of all components are related to increases in the radio flux. They do not, however, provide a quantitative assessment of this relationship. Flux increases are indeed expected to be associated with the appearance of new jet components if these are new ejecta that become optically thin as they move away from the core. A further possible link has been established by (Krichbaum et al. 1996) between the ejection of the knots and the high energy activity of 3C 273 as evidenced by ECRET data.

The VLBI observations quoted in (Krichbaum et al. 1990) were made at 43 GHz. VLBI observations at even higher frequencies (100 GHz) were obtained by (Bååth et al. 1991). These data reach a resolution of 50 micro seconds of arc, illustrating the power of the technique. Using  $H_0 = 50 \text{ km/(s Mpc)}$  this angular resolution corresponds to a linear scale of  $5 \cdot 10^{17} \text{ cm}$  at the distance of 3C 273. This is to be compared with the gravitational radius of a  $10^{10}$  solar masses black hole, which is  $3 \cdot 10^{15} \text{ cm}$ . In other words, modern VLBI observations are capable of resolving structures in the radio data of 3C 273 down to 100 gravitational radii. This effort to obtain maps at higher frequencies is being pursued (see e.g. (Krichbaum et al. 1997)).

High angular resolution VLBI data reveal that the angle at which the jet emerges from the core is significantly different at the hundred micro arcsecond scale ( $-119^\circ$ ) from that observed at the mili arcsecond scale ( $-130^\circ$ ) or at longer scales ( $-137^\circ$ )

(Bååth et al. 1991) and references therein). (Bååth et al. 1991) interpret this result as being due to either deflection of the jet or (but this is in a sense equivalent) to changes in the speed of the jet. This must be put in parallel with the observation of (Krichbaum et al. 1990) who report that the velocities of the individual knots are different (from  $4 \pm 0.3$  to  $8 \pm 0.2$  times the velocity of light).

Another type of improvement in the knowledge of the jet was brought about by investigations with a higher dynamical range. Such observations are reported in (Davis Unwin & Muxlow 1991). Two important results follow from their data. The superluminal motions observed at small distances from the core extend to at least 240 pc ( $H_0 = 50 \text{ km}/(\text{s} \cdot \text{Mpc})$ ). The velocity at large distances is only marginally less than closer to the core. The second result is that no counter jet is detected. The brightness ratio between a jet and an intrinsically identical counterjet is given by

$$[(1 + \beta \cos \theta)/(1 - \beta \cos \theta)]^{2+\alpha}.$$

Using a spectral index of 0.8 (Davis Unwin & Muxlow 1991) deduce from the observed lower limit on this ratio that  $\beta \geq 0.95$ . This velocity is close to that obtained from the superluminal expansion (see below). The data available is therefore still compatible with the presence of a counter jet of similar properties to the one observed but unobserved due to its relativistic motion away from us. A further improvement of the dynamical range by a factor of a few would provide an important set of data on the intrinsic properties of an eventual counter jet.

The intrinsic velocity of a relativistic jet can be deduced from the apparent proper motion in the following way (the original model is due to (Blandford McKee & Rees 1977)):

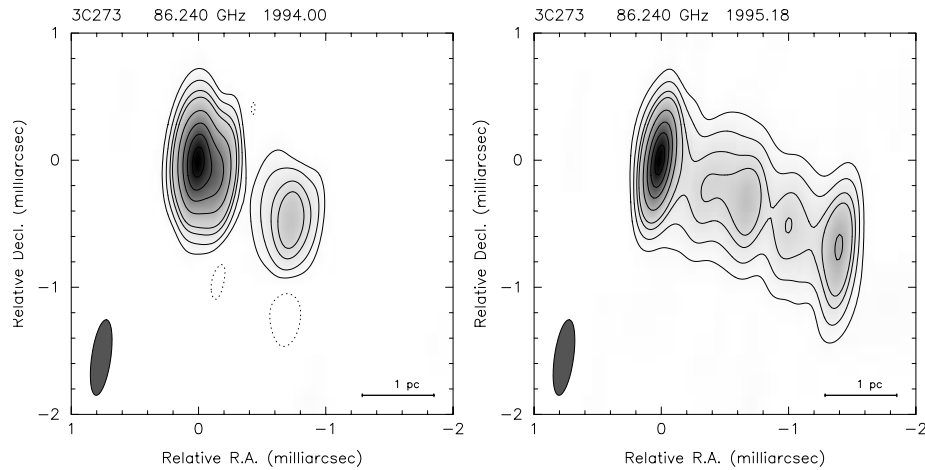


**Fig. 12.** The VLBI Jet of 3C 273 at two different epochs in 1994 and 1995 observed at 86 GHz. (courtesy T. Krichbaum.)

Assume that a photon is emitted by a blob of the jet that has traveled during  $\delta t$  at the velocity  $v$ . The difference in arrival time of this photon and one that originated from the base of the jet at the time of departure of the blob  $\Delta t$  is

$$\Delta t = \delta t(1 - v/c \cos \theta).$$

The motion of the blob a perpendicular to the line of sight seen by an observer far away is

$$v_{\perp} = \frac{\delta t v \sin \theta}{\Delta t}.$$

It is easily seen from both expressions that superluminal motion can be observed for  $v$  close to  $c$  and  $\cos \theta$  close to one and that the angle  $\theta$  for which the transverse velocity is maximum for a given intrinsic velocity is given by

$$\cos \theta_{max} = v/c.$$

## 7. The host galaxy

If there is one subject for which the brightness of 3C 273 is a problem rather than a help it is the study of the underlying galaxy. Subtraction of the quasar light distribution on images has proved a very delicate issue and has been possible only after the introduction of CCD cameras. (Kristian 1973) followed the idea that the quasar phenomenon is similar in nature to that observed in the nuclei of Seyfert galaxies but considerably more powerful and studied whether galaxies can be seen around at least some quasars in direct photographic plates. He concluded that in some cases galaxies are seen while for the brighter objects (including 3C 273) this is not the case, a conclusion expected from the quality of the data.

First (to my knowledge) CCD images of 3C 273 are presented by (Tyson Baum & Kreidl 1982). These authors conclude that there is an underlying galaxy and that it is similar to the giant elliptical galaxy NGC 4889 in the Coma cluster. The integrated V magnitude of the nebulosity is about 16.05, 3 magnitudes less than the quasar. Based on some previous data on the field of 3C 273 by (Stockton 1980) they also concluded that the 3C 273 host galaxy may be a member of a poor cluster of galaxies.

Near infrared data may be of interest to study the galaxies around quasars as the ratio of galaxy to QSO fluxes may be in general larger than at visual wavelengths (quasars are blue objects). (Veron-Cetty & Woltjer 1990) show thus that for luminous quasars there is no correlation between the luminosity of the galaxy and that of the QSO. (McLeod & Rieke 1994) present a sample of high luminosity quasars including 3C 273. They show that there is in their sample some correlation between the QSO luminosity and that of the underlying galaxies, 3C 273 having the most luminous underlying galaxy of their sample and the smallest fraction of galaxy to (QSO+galaxy) luminosity. The correlation shows, however, a large dispersion. Using far infrared luminosities, (McLeod & Rieke 1994) also investigate the possible existence of starburst activity in the galaxies surrounding quasars. They (preliminarily) conclude that this may be excluded in several of the galaxies, not in all and in particular not in 3C 273.

HST data have recently been published by (Bahcall et al. 1997) for a sample of nearby luminous quasars. The main advantage of the (repaired) HST is, expectedly, the sharpness of its point spread function that allows a cleaner subtraction of the quasar light from the image. This still requires, however, a good knowledge of the point spread function at some distance from the central peak, where the galaxies contribute most of their light. It is interesting to see that the HST data is in contradiction with the popular idea that radio loud quasars lie in bright elliptical galaxies while the radio quiet quasars, like Seyfert nuclei, lie in spiral galaxies. We can conclude from this

that it is not the obvious shape of the galaxy that determines the characteristics of the quasar.

In the case of 3C 273, the inferences drawn from the HST data confirm those obtained from the ground. The galaxy may be classified as an E4 galaxy, its luminosity is roughly 3 magnitudes fainter than the quasar in the visible. This indicates that the galaxy is somewhat brighter than the most luminous galaxy of a rich cluster. There is no conspicuous companion or signs of recent violent interaction with another galaxy. The galaxy major axis is about  $30''$ , corresponding to some 100 kpc with the cosmological parameters used here.

Whereas the study of a single object cannot have universal value, it is still interesting to note that 3C 273, the brightest nearby quasar, is not imbedded in a distorted or peculiar galaxy. This shows that while galaxy interactions may play an important role in bringing material from the galaxy to its nucleus, some other mechanisms must also be at work and even have the dominant role in at least some very bright cases.

## 8. Understanding it

The paradigm of QSO physics is that the energy is freed by accretion of matter in a massive black hole. This paradigm allows some simple estimates:

The Eddington luminosity for which gravitational attraction compensates radiation pressure is:

$$L_{Edd} = 1.3 \times 10^{38} \frac{M}{M_{\odot}} \text{ergs/s.}$$

Using the bolometric luminosity of 3C 273 deduced in Sect. 3.5 we thus estimate that provided that the bulk of the luminosity is emitted isotropically the mass of the central black hole is  $\sim 10^9$  solar masses. The corresponding gravitational radius is  $\sim 3 \cdot 10^{14}$  cm.

The mass accretion rate can be estimated from the luminosity  $L$  by:

$$L = \eta \cdot \dot{M} c^2,$$

where  $\eta$  is the efficiency of the conversion of rest mass to radiation.

Using the same luminosity as above and an efficiency  $\eta \sim 10\%$  typical of accretion onto black holes we deduce a mass accretion rate  $\dot{M} \sim 1.3 \cdot 10^{27} \text{ g s}^{-1}$  or about 10 solar masses per year. Not surprisingly, these numbers are close to those deduced from accretion disc models.

Going beyond these estimates requires understanding of how the energy liberated by the accretion process is transformed in the radiation we observe across the electromagnetic spectrum. This understanding is still widely lacking, we can, however, list some of the elements that do play a role.

Highly relativistic electrons and magnetic fields must belong to any model of 3C 273 (and other radio loud AGN) as shown by the presence of synchrotron radiation. Their energy densities are very inhomogenous and partly organized in small packets some of which at least are accelerated to relativistic bulk velocities along complex paths to form the observed small scale jet. It is probable that the electrons are accelerated to highly relativistic energies in shocks and that they thus acquire the energy that they radiate from the kinetic energy of some underlying flows.

Another indication of fast flows is the presence of the broad lines which indicate that the material surrounding the black hole has velocities of the order of  $10^4$  km/s.

It has not been possible to find in the line variability pattern the signature for a dominantly ordered velocity field (expansion, accretion or rotation). One, therefore, concludes that a large fraction of the velocity field is of a turbulent nature. In these circumstances, the presence of shocks where streams of matter collide is difficult to avoid. It is interesting to note that thermalising Hydrogen gas with bulk velocities of the order of  $10^4$  km/s will produce a gas of  $T \sim 5 \cdot 10^9$  K. A temperature close to the one needed to Comptonise the UV photons to X-rays with a slope as observed (Walter & Courvoisier 1992).

A fraction of the UV and higher energy radiation is reprocessed by gas to form the broad lines and by dust to give the thermal infrared radiation. The organisation of the broad line emitting clouds is unclear, no cloud confining medium having been found. Whether the optical-UV emission forming the blue bump is itself due to reprocessed X-ray emission is also unclear, mostly because of the absence of the signature of Compton reflection in the X-rays.

There are many different timescales at play. Among those we know there is the few days delay between the UV and optical light curves which imply that the signals ruling the blue bump emission travel at the speed of light. There is also the presence of much longer timescales (of several years) in the visible light curves and correlations which delays of the order of a year or so, between emission components. These timescales are long compared with light crossing times or dynamical times in the vicinity of the black hole. They are, however, short compared to viscous timescales of standard accretion discs. (Courvoisier & Clavel 1991). The presence of these timescales may either indicate that the size of the continuum emitting accretion is of the order of a parsec (similar to the size of the broad line region) or that there exist characteristic velocities of the order of few percent of the speed of light in a region of several gravitational radii. One may also note that the amplitude of the variations at short timescales (one day  $\sim 10$  gravitational radii over  $c$ ) is small (few percent; (Paltani et al. 1998)). This may indicate that the variations on this timescale are not associated with the regions closest to the black hole, but rather to small regions in an extended object.

There have been many attempts to understand the geometry of the emission regions considering one or several emission components. Most have been based on the presence of accretion discs. Many of the arguments are reviewed in (Blandford 1990). The addition of a corona being discussed by (Haardt et al. 1994).

(Camenzind & Courvoisier 1983) attempted to understand the continuum emission of 3C 273 in terms of a mildly relativistic wind originating in the core of the object and shocked at some distance. Most of the observed emission in this model was the by product of the shocked material. This model predicted that the variation time scales of the different components was such that the UV varied faster than the X-rays which in turn varied faster than the optical emission. The infrared and gamma ray variability timescales were expected to be the longest. These predictions were soon disproved by observations which led to a revision of the geometry (Courvoisier & Camenzind 1989). In this revised geometry the wind is channeled in such a way that the shocked material covers only few percents of the UV source. The shocked material is heated to temperatures such that the UV photons crossing it are Comptonised to X-ray energies. The lag between X-ray and UV fluxes may be understood naturally in this geometry (Paltani et al. 1998).

(Courvoisier et al. 1996) have considered whether accretion of matter could be in the form of stars rather than gas. In their model the gravitational energy is radiated following collisions between stars in the vicinity of a black hole. First order consid-

erations showed this to be a possible alternative to understand the variability of AGN and its dependence on luminosity. This also points to the little studied question of the interaction between the active nucleus and the surrounding stellar population.

It is thus clear that although the main elements of the AGN model have been in place for more than 30 years, often following pioneering observations of 3C 273, much remains to be understood. AGN are considerably more complex than many of us anticipated. This complexity together with the extreme properties they show make them fascinating object to study.

*Acknowledgements.* This work is based on a long term effort by a large set of colleagues who have participated in the gathering of data and in many discussions over the years. I owe a particular debt to M. Camenzind and M.-H. Ulrich for sharing their knowledge with me when this effort began. I would never have been able to write this review without the benefit from many interactions over the years and around the world. Several of my colleagues at the ISDC have given me some very direct help in preparing this review and in particular the figures. They are S. Paltani, M. Polletta and M. Türler. I thank them and also T. Krichbaum, R. Walter and L. Woltjer for reading and commenting the manuscript. A. Aubord and M. Logossou have been of much help in the typesetting.

## References

- Abraham Z., Carrara E.A., Zensus J.A. and Unwin S.C., 1996, *A&AS* 115, 543  
 Allen D.A., 1980, *Nat* 284, 323  
 Aller H.D., Aller M.F., Latimer G. and Hodge P.E., 1985, *ApJS* 59, 513  
 Bååth L.B., Padin S., Woody D. et al., 1991, *A&A* 241, L1  
 Angione R.J. and Smith H.J., 1985, *AJ* 90, 2474  
 Bahcall J.N., Kirhakos S., Schneider D.P., Davis R.J., Muxlow W.B., Garrington S.T., Conway R.G. and Unwin S.C., 1995, *ApJ* 452, L91  
 Bahcall J. N., Kirhakos S., Saxe D. and Schneider D.P., 1997, *ApJ* 479, 462  
 Bassani L., Jourdain E., Roques J.-P., et al., 1992, *ApJ* 396, 504  
 Bignami G.F. et al., 1981, *A&A* 93, 71  
 Binette L., Courvoisier T.J.-L. and Robinson A., 1988 *A&A* 190, 29  
 Blandford R.D., in *Active Galactic Nuclei*, Blandford, Netzer and Woltjer, Saas Fee Advanced Course 20, Springer Verlag  
 Blandford R.D., McKee C.F. and Rees M.J., 1977, *Nat* 267, 211  
 Bowyer C.S., Lampton M. and Mack J., 1970, *ApJ Letters* 161, L1  
 Broten N.W., Locke J.L., Legg T.H., Mc Leish C.W., Richards R.S., Chisolm R.M., Gush H.P., Yen J.L. and Galt J.A., 1967, *Nat* 215, 38  
 Burbidge E.M., 1967, *ARA&A* 5, 399  
 Burbidge G. and Burbidge M., 1967, *Quasi Stellar Objects*, Freeman and Company San Francisco  
 Camenzind M. and Courvoisier T.J.-L., 1983, *ApJ* 266, L83  
 Camenzind M. and Courvoisier T.J.-L., 1984, *A&A* 140,341  
 Clark B.G., Cohen M.H. and Jauncey D.L., 1967, *ApJ Letters* 149, L151  
 Clements S.D., Smith A.G., Aller H.D. and Aller M.F., 1995, *AJ* 110, 529  
 Cohen M.H., Cannon W., Purcell G.H., Shaffer D.B., Broderick J.J., Kellermann K.I. and Jauncey D.L., 1971, *ApJ* 170, 207.  
 Cohen M.H., Kellermann K.I., Shaffer D.B., Linfield R.P., Moffet A.T., Romney J.D., Seilstad G.A., Pauliny-Toth D.B., Preuss E., Witzel A., Schilizzi R.T. and Geldzahler B.J., 1977, *Nat* 268, 405  
 Cohen M.H., Pearson T.J., Readhead A.C.S., Seielstad G.A., Simon R.S. and Walker R.C., 1979, *ApJ* 231, 293.  
 Collin-Souffrin S. and Lasota J.-P., 1988, *PASP* 100, 1048  
 Conway R.G., Garrington S.T., Perley R.A. and Biretta J.A., 1993, *A&A* 267, 347  
 Courvoisier T.J.-L. and Ulrich M.-H., 1985, *Nat* 316, 554  
 Courvoisier T.J.-L., 1988, in *Variability of Blazars*, Eds E. Valtaoja and M. Valtonen, Cambridge University Press p. 399

- Courvoisier T.J.-L., 1997 in the proceedings of "All sky X-ray observations in the next decade", Eds Matsuoka M. and Kawai N., p. 207.
- Courvoisier T.J.-L., 1998 to appear in the proceedings of IAU joint discussion 18, Eds Courvoisier and Trimble
- Courvoisier T.J.-L. and Camenzind M., 1989, A&A 224, 10
- Courvoisier T.J.-L. and Clavel J., 1991, A&A 248, 389
- Courvoisier T.J.-L., Turner M.J.L., Robson E.I., Gear W.K., Staubert R., Blecha A., Bouchet P., Falomo R., Valtonen M. and Teräsraanta H., 1987, A&A 176, 197
- Courvoisier T.J.-L., Robson E.I., Blecha A., Bouchet P., Hughes D.H., Krisciunas K. and Schwarz H., 1988, Nat 335, 330.
- Courvoisier T.J.-L., Robson E.I., Blecha A., et al., 1990, A&A 234, 73
- Courvoisier T.J.-L., Paltani S. and Walter R., 1996, A&A 308, L17
- Czerny B., 1994, in Multi-wavelength continuum emission of AGN, IAU Symp. 159, Eds Courvoisier and Blecha, Kluwer academic publishers
- Davis R.J., Unwin S.C. and Muxlow T.W.B., 1991, Nat 354, 374
- Dent W.A., 1965, Sci 148, 1458
- Friedman H. and Byram E.T., 1967, Sci 158, 257
- Grandi P., Guainazzi M., Mineo T., et al., 1997, A&A in press
- Greenstein J.L. and Schmidt M., 1964, ApJ 140, 1
- Gursky H. and Schwartz D.A., 1977, ARA&A 15, 541
- Haardt F., Maraschi L. and Ghisellini G., 1994, ApJ 432, L95
- Harris D.E. and Stern C.P., 1987, ApJ 313, 136
- Hazard C., MacKey M.B. and Shimmins A.J., 1963, Nat 197, 1037
- Hughes P.A., Aller H.D. and Aller M.F., 1992, ApJ 369, 469
- Hyland A.R., Becklin E.E. and Neugebauer G., 1978, ApJ Letters 220, L73
- Kellog E., Gursky H., Leong C., Schreier, Tanabaum H. and Giacconi R., 1971, ApJ Letters 165, L49
- Knight C.A., Robertson D.S., Rogers A.E.E., Shapiro I.I., Whitney A.R., Clark T.A., Goldstein R.M., Marandino G.E. and Vandenberg N.R., 1971, Sci 173, 52
- Krichbaum T.P., Booth R.S., Kus A.J. et al., 1990, A&A 237, 3.
- Krichbaum T.P., Witzel A., Graham D.A., Lobanov A.P., 1996, in MM-VLBI Science Workshop, eds R. Barvainis and R.B. Phillips
- Krichbaum T.P., Witzel A., Graham D.A., Greve A., Wink J.E., Alcolea J., Colomer F., de Vicente P., Baudry A., Gomez-Gonzalez J., Grewing M. and Witzel A., 1997, A&A 323, L17
- Kristian J., 1973, ApJ 179, L61
- Krolik J.H. and Kallman T.R., 1988, ApJ 324, 714
- Leach C.M., McHardy I.M.M. and Papadakis I.E., 1995, MNRAS 272, L221
- Lelièvre G., Nieto J.-L., Horville D., Renard L. and Servan B., 1984, A&A 138, 49.
- Lichti G.G., Balonek T., Courvoisier T.J.-L. et al., 1995, A&A 298, 711
- Maisack M., Kendziorra E., Mony B., et al., 1992, A&A 262, 433
- Malkan M.A., 1983, ApJ 268, 582
- Malkan M. and Sargent W.L.W., 1982, ApJ 254, 22
- Mannheim K., 1993, A&A 269, 67
- Mannheim K., 1994, in Multi-wavelength Continuum emission of AGNp. 285, Eds. Courvoisier and Blecha
- Marcowith A., Henri G. and Pelletier G., 1995, MNRAS 277, 681
- Marscher A.P. and Gear W.K., 1985, ApJ 298, 114
- Marshall N., Warwick R.S., and Pounds K.A., 1981, MNRAS 194, 987
- McLeod K.K. and Rieke G.H., 1994, ApJ 431, 137
- McNaron-Brown K., Johnson W.N., Jung G.V., et al., 1995, ApJ 451, 575
- von Montigny C., Aller H., Aller M. et al., 1997, ApJ 483, 161
- Mushotzky R.F., Done C. and Pounds K.A., 1993, ARA&A 31, 717
- Netzer H., in Active Galactic Nuclei, Blandford, Netzer and Woltjer, Saas Fee Advanced Course 20, Springer Verlag
- Neugebauer G., Oke J.B., Becklin E.E. and Mathews K., 1979, ApJ 230, 79
- O'Brien P.T., Zheng W. and Wilson R., 1989, MNRAS 240, 741
- Pacholczyk A.G. and Weymann R.J., 1968, AJ 73, 870
- Paltani S., 1995, PhD. Thesis University of Geneva
- Paltani S. and Walter R., 1996, A&A 312, 55
- Paltani S., Courvoisier T.J.-L., Türler M. and Walter R., 1998, submitted

- Pearson T.J., Unwin S.C., Cohen M.H., Linfield R.P., Readhead A.C.S., Seilstad G.A., Simon R.S. and Walker R.C., 1981, *Nat* 290, 365
- Peterson B.M., 1993, *PASP* 105, 247
- Peterson B.M., 1997, *An Introduction to Active Galactic Nuclei*, Cambridge University Press
- Readhead A.C.S., Pearson T.J., Cohen M.H., Ewing M.S. and Moffet A.T., 1979, *ApJ* 231, 299.
- Rieke G.H. and Lebofsky M.J., 1979, *ARA&A* 17, 477
- Robson E.I., Gear W.K., Clegg P.E., Ade P.A.R., Smith M.G., Griffin M.J., Nolt I.G., Radostitz J.V. and Howard R.J., 1983, *Nat* 305, 194
- Robson E.I., Gear W.K., Brown L.M.J., Courvoisier T.J.-L., Smith M.G., Griffin M.J. and Blecha A., 1986, *Nat* 323, 134
- Robson E.I., Litchfield S.J., Gear W.K. et al., 1993, *MNRAS* 262, 249
- Roeser H.-J. and Meisenheimer K., 1991, *ApJ* 252, 458
- Roeser H.-J., Conway R.G. and Meisenheimer K., 1996, *A&A* 314, 414
- Roeser H.-J., Meisenheimer K., Neumann M. and Conway R.G., 1996, *MPE report* 263, 499
- Roeser H.-J., Meisenheimer K., Neumann M., Conway R.G., Davis R.J. and Perley R.A., 1997, *Reviews in Modern Astronomy* 10, 253
- Salpeter E.E., 1964, *ApJ* 140 796
- Schmidt M., 1963, *Nat* 197, 1040
- Schmidt M., 1969, *ARA&A* 7, 527
- Shakura N. and Sunyaev R., 1973, *A&A* 24, 337
- Sharov A.S. and Efremov Yu. I., 1963, *Intern. Bull. Var. Stars*, No 23 (Com. 27, IAU)
- Shields G.A., 1978, *Nat* 272, 706
- Shklovsky I.S., 1964, *Soviet Astron. AJ* 8, 638
- Smith H.J. and Hoffleit D., 1963, *Nat* 198, 650
- Stockton A., 1980, *IAU Symposium* 92, eds G.O. Abell and P.J.E. Peebles, Reidel, p.94
- Swanenburg B.N. et al., 1978, *Nat* 275, 298
- Teräsraanta H., Tornikoski M., Valtaoja E., et al., 1992, *A&AS* 94, 121
- Tornikoski M., Valtaoja E., Teräsraanta H., Smith A.G., Nair A.D., Clements S.D. and Leacock R.J., 1994, *A&A* 289, 673
- Türler M. and Courvoisier T.J.-L., 1997, *A&A* in press
- Türler M., Paltani S., Courvoisier T.J.-L., et al., 1998, *A&A Supp.*, in press
- Turner M.J.L.T., Williams O.R., Courvoisier T.J.-L., et al., 1990, *MNRAS* 244, 310
- Tyson J.A., Baum W.A. and Kreidl T., 1982, *ApJ*, 257, L1
- Ulrich M.-H., 1981, *Space Science Reviews* 28, 89
- Ulrich M.-H., Courvoisier T.J.-L. and Wamsteker W., 1988, *A&A* 204, 21
- Ulrich M.-H., Courvoisier T.J.-L. and Wamsteker W., 1993, *ApJ* 411, 125
- Veron-Cetty M.P. and Woltjer L., 1990, *A&A* 236, 69
- Veron-Cetty M.P. and Veron P., 1995, *A catalogue of Quasars and AGN*, 7th edition. ESO Report.
- Walter R. and Courvoisier T.J.-L., 1992, *A&A* 258, 255
- Walter R. and Fink H.H., 1993 *A&A* 274, 105
- Walter R., Orr A., Courvoisier T.J.-L., Fink H.H., Makino F., Otani C. and Wamsteker W., 1994, *A&A* 285, 119
- Waltman E.B., Fiedler R.L., Johnston K.J., Spencer J.H., Florkowski D.R., Josties F.J., McCarthy D.D. and Tatsakis D.N., 1991, *ApJS* 77, 379
- Wilkes and Elvis, 1987, *ApJ* 323, 243
- Willingale R., 1981, *MNRAS* 194, 359.
- Wills B.J., Netzer H. and Wills D., 1985, *ApJ* 288, 94
- Yaqoob T., Serlemitsos P., Mushotzky R., et al., 1994, *PASJ* 46, L49
- Zel'dovich Ya. B. and Novikov D., 1964, *Sov. Phys. Dokl.* 158, 811